A Test of the Biogenicity Criteria Established for Microfossils and Stromatolites on Quaternary Tufa and Speleothem Materials Formed in the "Twilight Zone" at Caerwys, U.K.

A.T. Brasier[1*], M.R. Rogerson[2], R. Mercedes-Martin[2], H.B. Vonhof[3] and J.J.G. Reijmer[3].

1*: Corresponding Author: School of Geosciences, Meston Building, University of Aberdeen, Old Aberdeen, Scotland, UK. AB24 3UE. Email: a.brasier@abdn.ac.uk; Telephone: +44(0)1224 273 449; Fax: +44(0)1224 278 585.

2: Department of Geography, Environment and Earth Science University of Hull Cottingham Road, Hull, UK. HU6 7RX

3: Faculty of Earth and Life Sciences, VU University Amsterdam, De Boelelaan 1085, 1081HV, Amsterdam, The Netherlands

Running title: Biogenicity of tufa stromatolites

18

Abstract

The ability to distinguish the features of a chemical sedimentary rock that can only be attributed to biology is a challenge relevant to both geobiology and astrobiology. This study aimed to test criteria for recognizing petrographically the biogenicity of microbially influenced fabrics and fossil microbes in complex Quaternary stalactitic carbonate rocks from Caerwys, UK. We found that the presence of carbonaceous microfossils, fabrics produced by the calcification of microbial filaments, and the asymmetrical development of tufa fabrics due to the more rapid growth of microbially influenced laminations could be recognized as biogenic features. Petrographic evidence also indicated that the development of ”speleothem-like” laminae was related to episodes of growth interrupted by intervals of non-deposition and erosion. The lack of any biogenic characteristics in these laminae is consistent with their development as a result of variation in the physico-chemical parameters that drive calcite precipitation from meteoric waters in such environmental settings.

Key words: microfossil, stromatolite; biogenicity; carbonate; tufa; speleothem

Introduction

The ability to distinguish those features of a chemical sedimentary rock that can only result from biology has proven to be a challenge for carbonate deposits (e.g., Wright and Barnett, 2015). As such an aim is essential for astrobiology and geobiology research (e.g., Cady and Noffke, 2009), we tested the ability to recognize signs of life and identify fossilized microbiota in Quaternary tufas and speleothem materials with the use of biogenicity criteria developed to recognize ancient microfossils (Sugitani et al., 2007; Wacey, 2009) and stromatolites (Buick et al., 1981; Hofmann, 2000). Of particular relevance to life detection in carbonates is the issue of a boundary that has been somewhat arbitrarily drawn between "speleothem" terrestrial carbonate rocks that form in dark caves, typically consisting of coarse columnar crystals that grow at rates of up to around 100 microns per year and are assumed to be essentially abiotic (e.g., Fairchild et al., 2006; Frisia and Borsato, 2010), and spring and stream "tufa" carbonate rocks. The latter are very similar to speleothem carbonate rocks, but they form in spring, stream and lake settings where photosynthetic cyanobacteria, algae and plants abound (e.g., Andrews and Brasier, 2005; Brasier et al., 2010) and are most commonly comprised of small "micritic" calcite crystals. Unlike speleothems, tufas are increasingly presumed to be biotically influenced (e.g., Freytet and Verrecchia, 1998; Arp et al., 2001; Pedley, 2014). Tufas grow more rapidly than speleothems, at rates of several millimeters to centimeters per year. There is

increasing recognition that tufa and speleothem systems form part of a continuum that also includes hydrothermal "travertines" (Rogerson et al., 2014), which suggests that some aspects of speleothem growth are likely to be enhanced by microbial growth in some instances (Cacchio et al., 2004).

To test whether existing biogenicity criteria for microfossils and stromatolites could distinguish biotic from abiotic features in chemical sedimentary precipitates, we applied them to the potentially complex specimens that grow in the so-called "twilight zone" at the entrance to modern caves (see Jones, 2010), and in caverns of Quaternary tufa deposits. Carbonate rocks that formed in a twilight zone where there is a transition from tufa to speleothem carbonate rocks include the Holocene barrage tufa deposit located at Caerwys, north Wales, UK (Figs. 1 and 2; Pedley, 1987). This tufa deposit contains several meter-scale cavities or caverns that are locally decorated with speleothem-like stalactitic calcite. The cavities are a primary feature that formed behind "curtains" of petrified moss that draped over tufa dams known as "barrages" (Figs. 2 and 3). We examined whether characteristics of the fabrics of specimens that formed in these twilight zone conditions could be differentiated from those formed biotically under the influence of photosynthesisers ("tufa-like"), and those formed abiotically in the dark ("speleothem-like"). We also determined which

petrographic criteria developed for distinguishing biotic from abiotic precipitates were most successful when applied to these Holocene specimens, with potential implications for early Earth studies and astrobiology searches.

Abiotic vs biotic origins of tufas and speleothems

Calcite precipitation in streams where tufas form was, until recently, most commonly viewed as a purely physico-chemical process (e.g., Zhang et al., 2001) in which CO_2 outgasses from fluids causing them to become supersaturated with respect to calcite, as reflected in the net thermodynamic equilibrium equation:

$$Ca^{2+} + 2HCO_3 <-> CaCO_3 + CO_2 + H_2O$$

CO_2 gas enrichment in meteoric waters occurs where they filter through biogenic CO_2-rich soil zones. The partial pressure of CO_2 builds in these environments so modern soil zone pCO_2 commonly considerably exceeds that of atmospheric CO_2. Calcite precipitation (Eq. 1) is typically associated with outgassing of this gas-rich fluid at spring effluents and where such fluids flow over obstacles like boulders or tree roots (e.g., Zhang et al., 2001). Recently this model has been challenged by Hammer and co-authors (2010) who found that dissolved gas concentrations decrease very little by turbulence caused by flow over surface irregularities, which led them to conclude that the most important role of turbulence was to

increase precipitation rates by bringing solutes to and from the calcite surface during turbulent mixing in the water column. Though the formation of stalactite and stalagmite speleothems in caves has most commonly been attributed to abiotic calcite precipitation driven by such physico-chemical processes (e.g., Frisia and Borsato, 2010), field studies (Freytet and Verrecchia, 1998; Vazquez-Urbez et al., 2009; Glunk et al., 2011) and laboratory experiments with viable biofilms collected from modern stream settings (Rogerson et al., 2008; Pedley et al., 2009) have demonstrated that both abiotic and biotic processes influence calcite precipitation in streams.

Recent experiments and field studies have also demonstrated that tufa precipitation can be significantly enhanced, even driven, by microbial extracellular polymeric substances (EPS) (e.g., Rogerson et al., 2008; Glunk et al., 2011; Pedley et al., 2014). The EPS of non-viable organisms has also been implicated in tufa formation (Rogerson et al., 2008). Biofilms of some species of cyanobacteria are reportedly associated with their own specific microfabrics (Freytet and Verrecchia, 1998), and such petrographic evidence would support the hypothesis that some cyanobacteria exert direct control on tufa formation.

Diagenetic alteration following deposition adds further complexity to the ability to determine the biogenicity of precipitated carbonate rocks like tufas and

speleothems. In spring or stream carbonate deposits, primary biofabrics may be rapidly overprinted and recrystallized generating textures that appear abiotic (Jones and Peng, 2012). For example, diagenetic changes transform primary tufas from finely crystalline (micritic) to more coarsely crystalline (sparry) calcite, the fabric changing either by aggrading neomorphism (Love and Chafetz, 1988; Janssen et al., 1999) or simply continued growth of favored crystals (Brasier et al., 2011). Yet characterizing all coarse, sparry calcite fabrics as either alteration products or abiotic would be an over-simplification (Brasier et al., 2011) that could lead to many microbial fossils, both ancient and modern, being overlooked.

Materials

The Caerwys tufa

The tufa deposit studied here was found to the south of the village of Caerwys in north Wales, UK (Figs. 1 and 2). The waters that formed the tufa were sourced from a spring in the Carboniferous limestone (Pedley, 1987). Tufa precipitation at Caerwys has been constrained via radiocarbon techniques to the Holocene and pre-Holocene 'Late Glacial' intervals (Preece and Turner, 1990). Deposition has now ceased but a small analogous active site is found nearby at Ddol (Preece and Turner, 1990). The Caerwys tufa forms a veneer of Quaternary terrestrial

carbonate rock over the underlying geology. It grew in a steep stream that flowed down the scarp-face of a Carboniferous Limestone outcrop, with a series of cascading pools developing behind arcuate tufa dams or "barrages" that were oriented transverse to flow (Fig. 2; Pedley, 1987). The Caerwys system would have resembled the currently active tufa-depositing stream at Alport, Derbyshire, UK (Fig. 3). In both cases (Caerwys and Alport) unconsolidated micrite muds are found in the pools between the barrages. Some of these pools contain isolated decimeter-scale thrombolitic heads constructed by calcifying cyanobacteria, green algae, and invertebrates. The barrage dams themselves comprise indurated but vuggy carbonate walls that include a similar assemblage of fossil organisms. Though extensively quarried, the internal fabric of the barrage system is visible (Fig. 2) and preserved as a site of special scientific interest (SSSI).

Lithostratigraphy and mollusc biostratigraphy of the quarry were described by Preece (1978; 1982) and a facies model was compiled by Pedley (1987). Tufa oxygen and carbon isotopes were detailed and their Quaternary climate implications discussed by Garnett et al. (2006). The latter estimated summer water temperatures were in the range of 13 to 16.5 $^{\circ}$C on the basis of tufa and gastropod $\delta^{18}O$ values.

Specimens exhibiting the continuum of tufas and speleothems

Pedley (1990) described calcitic tubes of tufa formed by fringe cements that encrusted larger plants (macrophytes). The samples analyzed in this study fit that basic description and calcite encrustations of macrophytes are identified by their morphology. Internally they have a central longitudinal cavity that may remain open or may have been filled by clastic grains (commonly but not necessarily of tufa carbonate) or calcite cement. They are differentiated from hollow abiotic stalactites such as "soda straws" in that they contain preserved carbonaceous matter or recognizable impressions of organisms that become encrusted when mineralized. In swampy paludal marshes and pool margins, most plant stems grow upwards and, when encrusted by carbonate, become stalagmite-like deposits (Pedley, 1990). In barrage systems, however, many plants including bryophytes live on the overhangs of the barrage (dam) front, their stems and branches hanging downwards. This leads to pendant, stalactite-like calcite-encrusted structures (Fig. 2). Externally these calcitic encrustations appear indistinguishable from "speleothem" stalactites or stalagmites formed in caverns. Encrustations may be <10 mm to several tens of centimeters in width, and range from a few centimeters to meters in length. Such encrustations are common but under-reported for modern karst settings. The oldest known examples may be the pendant cavity-filling cements of the 2.75 Ga Fortescue Group, Australia, which were interpreted as biogenic by Rasmussen et al. (2009).

Methodology

Eleven different tubular specimens from Caerwys, each several centimeters in length, were collected. All were examined in hand specimen and using standard petrographic microscopy techniques. Specimens were injected with blue resin, and both longitudinal and transverse thin-sections were prepared and analyzed. All rocks were found to be minimally or non-luminescent when viewed under UV light. Cathodoluminescence (CL) microscopy revealed that none of the specimens luminesced. Thin-sections were examined and photographed with the use of polarized light microscopy. Carbonaceous filaments entombed in calcite were distinguished from dark micritic calcite by partially dissolving the specimen with acetic acid. Similar petrographic histories were elucidated from all eleven specimens, such that we could select two representative specimens, labelled S3.2 and Caerwys 1, for detailed study.

Results

The descriptions of hand-specimen scale observations are followed by microscopic observations for specimen S3.2, followed by the same for specimen Caerwys 1. The terms micrite (crystals <4μm diameter), microspar (4 to 10μm

diameter), and spar (>10µm diameter) are used to indicate crystal sizes and do not reflect the origin of the grains.

Specimen S3.2: Hand-specimen scale observations

Specimen S3.2 is a downward-tapering stalactitic rock (Fig. 4) that was collected as a float specimen that was found adjacent to the central barrage outcrop in the quarry (Fig. 2b and 2c). Internally there is strong asymmetry, and at least six separate components of the visible fabric of the sample, referred to here as Zones 1-6, were delineated (Fig 5).

Zone 1 is located in the central section of the porous tufa, which is permeated by c. 50 to 100 µm diameter hollow tubes of calcite that form shrub-like growths oriented downward at around 55 degrees from horizontal (Fig. 4b). From examination of longitudinal and transverse sections it was possible to discern that these growths formed via micritic calcite encrustation of a biological (likely cyanobacterial) substratum. The asymmetrical nature of the sample, when viewed in cross-section, is due to the more extensive outward growth of this primary depositional fabric in one direction away from the point of initiation. Denser-looking white patches of tufa, developed on one (likely the upstream) side of this sample, cover an area around 3 mm across and a centimeter in length.

Zone 2 (Fig. 5) consists of micrite intergrown with dark brown sparry calcite fans, with the latter being dominant. Each fan is around 1 to 3 mm across, and all fans grew toward the outward edge of the specimen. This zone forms a band around 1 cm thick on one side of the specimen (the side toward which Zone 1 micrite prograded), and is traceable continuously around the perimeter, though it narrows to <1 mm thick on the opposite side of the sample.

Zone 3 in hand-specimen consists of a 1 to 2 mm thick light brown band that envelops calcite of Zone 2, and is capped by a darker brown 1 mm thick band. Internally these bands contain several very fine sub-mm thick cream colored laminae. These bands are thicker where they developed below cm-scale overhangs.

Zone 4 is recognizable in hand-specimen only as a white band that separates brown calcite below it from very similar-looking brown calcite above, which is designated as Zone 5. Note than Zone 4 appears brown in thin-section (Fig. 5).

Zone 6, the outer casing of the specimen, consists of a layer of cream colored botryoidal calcite, around 2 mm thick on one side and 6 mm thick on the other. This outer zone seems to be divided into two bands by a very thin dark lamina.

Specimen S3.2: Microscopy

Two thin-sections of sample S3.2 were made from the cut specimen. Scans of these are shown in Figure 4, one from the transverse sawn section (S3.2A) and the other from the longitudinal sawn section (S3.2B). Petrographic analysis of these thin sections confirmed that Zone 1 comprises 6.5 to 26 µm (mostly c. 20 µm) diameter dominantly sub-vertically oriented biological filaments that were encrusted by 18 to 50 µm thick walls of calcite (Figs. 4, 5 and 6a). The carbonaceous filaments themselves have mostly been oxidized, leaving behind empty calcite tubes (Figs. 6a and 7a), though some tubes contain carbonaceous material that resembles hollow and partially decomposed cyanobacterial trichomes within a sheath (Figs. 7b and c). The central parts of each calcite tube that would have been in contact with the carbonaceous filament are comprised of an envelope of small microcrystalline crystals. The remaining outer part of each calcite tube wall is constructed of radiating c. 20 µm diameter spar crystals (Fig. 7a). Also in Zone 1 is a cluster of hollow calcite tubes that ranged from 250 to 500 µm across (Fig. 7d). These each have an inner zone of microspar (crystals c. 20 µm diameter) followed by two rings of larger sparry crystals, each c. 45 µm thick. Some of these tubes have sparry calcite fan growths on one side, which marks the start of Zone 2.

The first Zone 2 sparry calcite fans (Figs. 4, 5 and 6a) nucleated directly on the spar of Zone 1 encrusted tubes. These two spar types are, in some locations, in optical continuity, which indicates that Zone 1 spar acted as a template for precipitation and growth of Zone 2 spar. Some curved, dark micritic growth lines within the fans are traceable between fans (Fig. 6a). Fans interfered with each other where they touched during growth. Some fans terminated in smooth curved surfaces; others were flat-topped (e.g. Fig. 8); and several exhibited pointed euhedral crystal terminations. Growth of Zone 2 seemingly ceased for extended periods of time (perhaps months?) on at least three occasions. These cessations are marked by dark micritic layers from which new fans nucleated. The latter are indicated by their different crystallographic orientations from the underlying fans (Fig. 6a). A magnified view of one of the Zone 2 fans, shown in Fig. 8, reveals that the carbonaceous filaments interpreted as entombed cyanobacteria are dominantly but not exclusively oriented sub-parallel to the direction of crystal growth. They are c. 2 μm wide and 40 μm long, distinctly narrower than the carbonaceous filaments of Zone 1. These narrower filaments cross through some of the finer, μm scale crystal growth bands within the fans (Fig. 8). The μm scale growth bands were likely formed on approximately diurnal timescales (Andrews and Brasier, 2005). Pedley (1987) suggested spar-entombed carbonaceous filaments of the Caerwys quarry could be *Schizothrix* or *Phormidium* sp. cyanobacterial fossils on the basis of growth form and diameter.

The contact between Zones 2 and 3 of this specimen (Figs. 4, 5, 6 and 9) is sharp in places though more transitional in others due the optical continuity of subsequent crystal growth. At its base, Zone 3 comprises numerous (at least six) couplets of micrite and columnar sparite (Fig. 9b). A micrite band c. 5 μm thick forms the nucleation region for numerous crystals of spar (mostly c.100 μm diameter) in several locations in the specimen. Petrography revealed that several of the latter columnar spar crystals, commonly with length to width ratios >6, developed through competitive growth of crystals that nucleated in this band (e.g., Figs. 9c and 9d). Other columnar crystals stem from lower horizons that include Zone 2 spar crystals (e.g., Fig. 9a). Inclusions in the columnar crystals appear as bands oriented perpendicular to the direction of growth and parallel to (and commonly in close proximity to) the bands of micrite (e.g., Fig. 9c and 9d). The inclusions were identified primarily within the calcite crystals rather than between them.

Most intriguing near the top of Zone 3 (Figs. 4, 5 and 10) is a patch a few mm across that includes a series of circular to oval pores that range from 100 to 240 μm in diameter (Fig. 10). The latter are most easily interpreted as transverse cross-sections of hollow tubes. One tube oriented longitudinally in the thin-section extends for at least 2.2 mm. At higher magnification it was determined

293 that the walls of these tubes are thinly lined with dark micrite, surrounded by
294 cylinders comprised of spar crystals 100 to 400 µm in diameter (Fig. 10c and
295 10d). The latter are differently aligned from the columnar calcite host, radiating
296 outward from the tube center. The crystals aligned parallel to the direction of
297 growth of the columnar spar are elongated upward, forming flame-like growth
298 shapes. These crystals evidently grew contemporaneously and in competition with
299 the surrounding columnar spar.

300 Zone 4 was recognized petrographically by the re-appearance of micrite on one
301 side of the specimen (Fig 5b). This zone is laterally traceable into spar via two c.
302 5 µm thick sub-parallel micritic bands that mark its top and bottom. The micrite
303 comprises a porous network of peloids that includes hollow tubes of c. 130 µm
304 diameter.

305 Zone 5 spar crystals terminations range from pointed to flat or broken and are
306 delineated by inclusions (see Fig 5 and Fig. 11). In places they are draped in
307 continuous bands of dark, dust-like micrite that infilled the depressions and
308 smoothed out the topography (Fig. 11a). Most spar crystals terminate at these
309 micrite layers, though this was not always the case (Fig. 11b). For example, in one
310 place a fragment of micrite 340 µm across adhered to the specimen surface (Fig.
311 11) and sits flat on a micritic layer. Spar crystals nucleated on this detrital micrite
312 inclusion, though they were later out-competed by other columnar crystals.

Further, the protrusion formed by this blob of micrite clearly affected development of the overlying layers (Fig. 11).

The tops of Zone 5 columnar crystals formed the substrate for Zone 6 crystal growth. Zone 6 crystals (Fig. 5 and Fig. 12) are distinctly different from those of Zone 5 and appear as networks of needle-like laths. The latter are arranged along the faces of a crystal lattice (Figs. 12a and 12b). These laths are sub-crystals (crystallites *sensu* Kendall and Broughton, 1978) that range individually in size up to c. 1 mm long and 50 µm wide and that link to form larger millimeter-to-centimeter scale composite crystals (Frisia and Borsato, 2010). These composite crystals are sometimes in optical continuity with the Zone 5 columnar calcite on which they grew (Fig. 12).

Specimen Caerwys 1: Hand-specimen scale observations

Caerwys 1 is an 8 cm long specimen that grew in a stalactitic fashion. It was collected from a cavern within *in situ* barrage deposits located in the center of the quarry. This specimen was collected from directly adjacent to the much larger stalactitic rock shown in Fig. 2c. In longitudinal section it was possible to recognize the sample has a highly porous center surrounded by several c. 0.5 to 1 mm thick layers that alternate with much thinner (c. 100 µm thick) lighter colored

layers (Fig. 13). At least three layers were traced in the specimen, though in places the layers appear to be merged or truncated.

Specimen Caerwys 1: Microscopy

A thin-section of Caerwys 1 was stained with Alizarin Red S and Potassium Ferricyanide. The pink color confirmed its non-ferroan calcite composition. The central cavity (Fig. 13) of this specimen is highly porous, evidenced by the blue resin (Fig. 14), and divided into several empty pockets by walls of sparry calcite. One empty pocket is lined with 20 μm diameter microspar crystals (Fig. 14a) that are partially intergrown and form a porous network. On both sides of this initial cavity fill are crystal fans of sparry calcite, with crystal lengths of 80 to 150 μm. Adjacent to the sparry calcite fans at the top of the specimen is a second empty pocket, 3 mm across, that was progressively filled by 300 μm diameter sparry calcite fans (Fig. 14b). These grew inwards from all sides toward the cavity center. Dark-colored inclusions within some of these fans are oriented along crystallite boundaries (Fig. 14c and 14d). The origin of these filamentous microfossil-like inclusions is discussed further below. The bulk of the specimen is comprised of layers of columnar sparry calcite that grew primarily outward as fans (Fig. 14e-g). Each crystal is c. 500 μm long and 50 to 100 μm wide. These sparry layers correspond to the thick, lighter colored layers observed in hand

specimen that are separated by laminae of micrite c. 130 μm thick (Fig. 13 and Fig. 14f). There is evidence that columnar sparry calcite fans were partially dissolved prior to or during deposition of the micrite layers (Fig. 14e), as some of the micrite layers are a little thicker (c. 230 μm) and more porous, particularly one layer close to the outside of the specimen (Fig. 14g).

Discussion

The criteria of Sugitani et al. (2007) and Wacey (2009) developed to establish the biogenicity of potential microbial fossils were applied to evaluate the biogenicity of the fossil-like objects in the two samples studied. For these specimens, their Quaternary age and sedimentary origins are not in doubt. These rocks have never been buried to any significant depth, so the characteristics of the precipitates and the fabrics were developed in the original sedimentary depositional environment.

Biotic vs abiotic growth of Specimen S3.2

A complex growth history of Specimen S3.2 was unravelled on the basis of the petrographic analysis, with different growth zones exhibiting different degrees of biotic influence. The oldest part of the specimen (in Zone 1; Figs. 5a and b) comprises dense, white colored calcitic tufa that contains clusters of hollow

carbonaceous tubes of fossilized cyanobacterial trichomes preserved inside sheaths. Zone 1 was formed by calcification of filamentous cyanobacterial shrubs that coated an overhanging leaf or twig. This photosynthesizing biofilm formed a substrate for subsequent growth that was necessarily focused away from the tufa wall toward the direction of light. Such biologically enhanced growth resulted in the asymmetrical, elongated form of the specimen. A network of 250 to 500 µm diameter hollow calcite tubes was formed by chironomid insect larvae, perhaps in the late Spring season as waters warmed up (Janssen et al., 1999; Brasier et al., 2011). Filamentous microbes coated these tubes, separated by at least one and possibly two or three pauses of unknown duration (perhaps weeks or months, likely at most a few years). Zones 1 and 2 are at least part contemporaneous, with Zone 2 sparry calcite shrubs containing thinner entombed carbonaceous filaments dominantly forming on the side of the specimen that received less light. Their presence on the more illuminated side of the specimen toward the end of Zone 1 deposition, including in small crevices, is consistent with the onset of shaded, lower light intensity conditions that supported the growth of microbial species associated with spar formation.

The Zone 1 microfossils must have been syngenetic with the calcite deposition, as the calcite initially developed as tubes nucleated on the filaments (Figs. 4, 5, 6a

391 and 7). It is possible that the Zone 2 microfossils (Fig. 8) represent endoliths that
392 bored into the tufa post-deposition, as they are oriented parallel to crystal growth
393 planes and cut across the micron-scale growth lines within the sparry calcite
394 crystal fans, features previously used as indicative of an endolithic habit (Knoll et
395 al., 2013). However the filaments in the Caerwys samples protrude across laminae
396 that likely formed on diurnal timescales, well within the lifetime of entombed
397 individual microorganisms. Further, endolithic organisms would also be expected
398 to target earlier formed tufa micrite as well as the crystal fans. The occurrence of
399 the Zone 2 filaments close to the center of the specimen and not in the outer parts
400 makes it unlikely that the cyanobacterial filaments preserved in Zone 2 were
401 endoliths. More likely, and as Pedley (1987) inferred, the filaments were
402 fossilized by syn-depositional calcite entombment.

403

404 Evidence for microbial influence on the growth of Zones 1 and 2, consistent with
405 the microfossil biogenicity criteria of Wacey (2009), includes:

406 1) Two different populations of carbonaceous filaments, each community
407 associated with its own characteristic carbonate rock microfacies and not
408 randomly distributed.
409 2) Entombed clusters of hollow brown-colored carbonaceous filaments that
410 are syngenetic with the carbonate rock. These microfossils include

411 sheathed trichomes and are comparable in size and morphology with
412 extant cyanobacteria.
413 3) Calcitic molds of colonies of microbial filaments preserved in the
414 carbonate rock, with calcification specifically on and around the filaments,
415 consistent with microbial influence on crystal nucleation.

416 Zone 3 (Fig. 9) lacks the microfossils of Zones 1 and 2 (Figs. 6, 7 and 8). The
417 thicker layering on the undersides of overhangs (Fig. 4b, 5b) is consistent with a
418 dominantly abiotic growth process. However, as in Zone 1, the 100 to 240 μm
419 diameter tubes (Fig. 10) are best interpreted as chironomid larval tubes (e.g.,
420 Brasier et al., 2011). Chironomid larvae are detrital feeders, which implies that
421 Zone 3 formed in detritus-rich flowing stream water. Tubes at the top of Zone 3
422 could be directly associated with the micrite of Zone 4. This inference is based on
423 the micritic peloids that could be of fecal origin, and additional tubes of likely
424 chironomid origin that occur in the Zone 4 micrite. This suggests that Zone 3 spar
425 and Zone 4 micrite are partly contemporaneous, and indeed Zone 4 micrite
426 merges laterally into sparry calcite.

427 Petrographic evidence that Zone 5 columnar spar is primary and not the result of
428 recrystallization includes the aggradational fabrics that surround the micrite
429 inclusion (Fig. 11). That the micrite inclusion sits flat on a thin micritic layer (Fig.
430 11a) is consistent with the latter representing a phase (perhaps a dry summer)

during which little calcite crystal growth occurred. New columnar crystals nucleated on top of the micrite (Fig. 11b), presumably during a wetter phase. The resulting topography caused deflection of the subsequent growth laminae. Ultimately the spar that nucleated on top of the micrite inclusion was out competed by the surrounding larger columnar crystals (Fig. 11b). Columnar spar of Zone 5 likely formed within or in very close proximity to the active tufa-depositing stream. These conditions could have been found behind the downstream facing accretionary surface of an actively accumulating tufa barrage. No obvious indicators of a biogenic cause for calcite deposition were identified in Zone 5. This does not necessarily imply that nucleation of Zone 5 spar was wholly abiotic: extracellular polymeric substances produced by microbes were very likely present in the stream water, though there was no direct evidence that they contributed to the formation of Zone 5 spar.

Similar to the crystals of the Zone 5 spar, the crystals of Zone 6 also lacked carbonaceous microfossils (Fig. 12). The fabric of Zone 6 was reminiscent of the open dendritic speleothem texture described by Frisia and Borsato (2010). Such textures are known to form at cave entrances, in places subject to kinetic processes such as prolonged degassing phenomena. Such a scenario is consistent with Zone 6 developing as a late-stage cave speleothem-like meteoric growth within the cavern. Unlike the within-stream conditions that supported the growth

of Zones 1-5, Zone 6 developed when the tufa stream system itself had become inactive.

In short, petrographic observations revealed that Zones 1 and 2 formed in the presence of microbes that included cyanobacteria; Zone 3 calcite growth was dominantly abiotic except for calcite tubes most likely constructed by chironomid larvae; Zone 4 is attributed to chironomid larvae that consumed microbes; there are no obvious preserved indicators of biological activity or control on calcite precipitation in Zone 5 and Zone 6, and the latter formed in different environmental circumstances compared to those that supported the growth of Zones 1 – 5. Abundant petrographic evidence for syn-depositional growth of columnar calcite spar is found in places with entombed cyanobacterial filaments (Zone 2), where crystal growth continued behind the aggrading outer surface layer (Fig. 6); where there is evidence of micrite bands capping spar layers, and competitive crystal growth of spar crystals (Fig. 9); where insect larval tubes are found in sparry calcite layers (Fig. 10); and where detrital micrite stuck to the specimen surface and interfered with growth of overlying spar crystals (Fig. 11). There is no evidence for recrystallization that would have required dissolution. Despite the presence of cyanobacteria in Zones 1 and 2, the most clearly laminated (i.e. “stromatolitic”) zones are 3 and 5 (Figs. 4 and 5). The latter are the most cave speleothem-like and arguably abiotic sections. This lamination is discussed further below.

Biotic vs abiotic character of Specimen Caerwys 1

Specimen Caerwys 1 is similar to specimen S3.2 in that it was nucleated on a downward hanging biological substrate, overgrown by successive layers of sparry calcite that extend to the outside of the sample. Caerwys 1 is a thinner specimen than S3.2. This may be partly due to absence of prograding cyanobacterial filaments in the core of Caerwys 1. Rather, the initial biological substrate seems to have been a stem or branch of a larger plant. The predominantly sparry calcite walls of Caerwys 1 are similar to Zone 2 of S3.2 (compare Figs 6b and 8 with Fig. 14c-f). Clusters of potential microfossil filaments in Zone 2 of specimen S3.2 (Fig. 8) and in the sparry calcite fans of Caerwys 1 (Fig. 14c) also share similar properties of size, coloring and orientation parallel to the direction of crystal growth. However, the orientation of the dark-colored Caerwys 1 filaments was directly related to the orientation of the crystal structure. A comparison of the observations against the biogenicity criteria of Sugitani et al. (2007) and Wacey (2009) indicate that the Caerwys 1 filaments are much less convincing as microfossil candidates than those found in the S3.2 sample.

Biogenicity of the lamination?

The specimens described here are layered carbonate rocks that by some definitions could be identified as “tufa stromatolites” (Riding, 1991) or simply stromatolites (e.g., Semikhatov et al., 1979). Therefore, to evaluate whether the Caerwys tufa layering would be identified as biogenic when commonly used stromatolite biogenicity criteria are applied, we used the criteria of Buick et al. (1981) and Hofmann (2000) as critiqued in McLoughlin et al. (2013).

The first group of biogenicity criteria pertain to the context of the lamination and include, for example, requirements that the structures be found in sedimentary or metasedimentary rocks and be syn-sedimentary with the deposit in which they are found. This is undoubtedly the case for these Quaternary tufas. Similarly, there is a criterion that brecciated mat chips should be found accumulated in depressions between convexly laminated mounds. Eroded chips of layered carbonate are found within the pool facies at Caerwys (Pedley, 1987). Such findings establish that the layered carbonate rocks are a primary sedimentary feature, but these contextual criteria do not differentiate biogenic from abiotic stromatolites.

The second group of biogenicity criteria pertain to the morphology of the lamination: a biogenic stromatolite should exhibit a preponderance of convex-upward structures; contain laminae that thicken over the crests of flexures; consist of laminations that are wavy, crinkled or have several orders of curvature; and

511 may be associated with thin, rolled-up fragments with coherent flexible laminae
512 that can reasonably be interpreted as microbial mats. However, none of these
513 criteria is itself diagnostic of a biogenic rock. Here we highlight, for example, that
514 several tufa stromatolites of cyanobacterial origin exhibit isopachous layering
515 (e.g., Janssen et al., 1999; Andrews and Brasier, 2005; Brasier et al., 2010; 2011).
516 Spar layers in Caeryws tufa specimen S3.2 Zone 3 that might otherwise be
517 interpreted as abiotic thicken over the crests of flexures, as do spar layers of Zone
518 5 (Fig. 11). Laminae of specimen Caerwys 1 seem thickest at the downward
519 pointing tip of the specimen (Fig. 13), which is consistent with the effects of
520 gravity and hence abiotic growth. Likewise, the thin micritic layers of Caerwys 1
521 are crinkled and curved (Fig. 13) yet the petrographic observations suggest that
522 these micrite bands are related to periods of exposure or non-deposition, as they
523 cap spar fans that are partially dissolved or eroded (Fig. 14e). Despite being
524 crinkled these micrite laminae are unlikely to be biogenic.

525

526 The third group of biogenicity criteria are those that relate to the nature of
527 microfossils and trace fossils within the lamination. Zones 1 and 2 of Specimen
528 S3.2 exhibit both entombed hollow carbonaceous filaments and calcitic external
529 molds of filaments oriented perpendicular to the lamination, not parallel to it.
530 Trace fossils of insect larvae are present within Specimen S3.2 Zone 3. It is

possible that these larvae were farming particular species of cyanobacteria above their tubes, and that the cyanobacteria influenced crystal growth. Alternatively the larvae might have produced their own growth-influencing organic substances (Brasier et al., 2011). However there is no evidence for microbes directly causing the lamination of Zone 3. Microfossils are notably absent in the most distinctly laminated section, Zone 5.

Additional biogenicity criteria require that changes in the composition of microfossil assemblages should be accompanied by morphological changes in biogenic stromatolites. Where more than one microfossil assemblage is present in the samples studied, changes in micromorphology were found in these specimens. For example, the narrow filaments of Specimen S3.2 Zone 2 are associated with sparry calcite fans (Fig. 8) whereas broader filaments in trichomes of Zone 1 are found in sub-vertically hanging tubes of calcite (Figs. 4, 5, 6 and 7).

The entombed microorganisms of Specimen S3.2 are also organized and clustered in a fashion consistent with colonial photoautotrophic growth. We infer that their EPS did not simply bind sediment (e.g., Gerbersdorf and Wieprecht, 2014) but that it actively assisted calcite crystal nucleation (Rogerson et al., 2008; Glunk et al., 2011). This hypothesis is supported by the petrographic evidence for preferential growth of the carbonate rock toward the most light-illuminated direction. Insect larval tubes present in the Caerwys tufa (Fig. 10) would

potentially meet a criterion that biogenic stromatolitic fossils must be organized in a manner that indicates trapping, binding or precipitation of sediment, though whether the insect larvae actively trapped, bound or precipitated the sediment themselves (e.g., Brasier et al., 2011) could not be discerned petrographically.

Though all of above criteria establish that the lamination is sedimentary in origin (Fig.6a) and the cyanobacterial microfossils are consistent with evidence for photoautotroph-induced specimen growth (see supplementary information S?), the cause of most of the lamination in the Caeryws specimens is related to alternating episodes of specimen growth, non-deposition and erosion (e.g., Figs. 9d, 11 and 14d). Physico-chemical parameters such as stream flow rates, pH, alkalinity, saturation and temperature likely controlled the development of such lamination. Though microbially produced EPS may have exerted some influence on the laminae microstructure, direct evidence for microbial control on the lamination was absent.

In summary, the criteria consistent with biogenic features in the layered tufas at Caerwys are those that relate to fossils of the organisms themselves, and not those of the lamination. Without the presence of microbial fossils, it would not be possible to identify the biogenicity of the laminae. Layering alone is not

570 diagnostic of a biogenic structure in specimens like those characterized in this
571 study.

572

573 **Implications for astrobiology**

574 Carbonate rocks that may be targets in the search for martian microfossils were
575 identified by Niles et al. (2013). As with Earth's deep time stromatolites
576 (McLoughlin et al., 2013), discriminating purely abiotic chemical sedimentary
577 precipitates from biogenic rock structures of Mars will prove challenging. It is
578 encouraging that simple criteria devised for ancient stromatolites and microfossils
579 (Buick et al., 1981; Hofmann, 2000; Sugitani et al., 2007; Wacey, 2009) here
580 enabled biogenic microfossils to be distinguished from abiogenic pseudofossils in
581 a complex terrestrial case.

582 It is worth noting that recognition of microfossils requires detailed microscopic
583 examination: definitively identifying biogenic structures in the examined
584 Caerwys specimens would not have been possible at the outcrop or hand-
585 specimen scales. Robotic exploration of Mars has already located potentially
586 habitable streams (Grotzinger et al., 2014), structures consistent macroscopically
587 with microbially-induced sedimentary structures have been described (Noffke,
588 2015), and chemical signals consistent with martian life (Webster et al., 2015)

589 have been reported. Potential lessons from the Caeryws quarry, however, are that
590 the microbial structures visible under the microscope are not readily identifiable
591 as biogenic at the hand-specimen scale, and the nature of the laminations were
592 such that they could not be proven as biogenic at the hand-specimen or
593 petrographic microscope scales.

594

595 **Conclusions**

596 The microfossils found in specimen S3.2 display at the petrographic scale the
597 most convincing evidence for biogenicity: the layered stalactitic rock developed
598 as a result of the calcification of filamentous cyanobacteria and different
599 populations of carbonaceous filaments were each associated with their own
600 characteristic carbonate rock microfacies.. The entombed clusters of hollow
601 filamentous carbonaceous microfossils that included sheathed cyanobacterial
602 trichomes demonstrated that the microfossil evidence is syngenetic with the
603 carbonate rock. The influence of biology on the morphology of the deposit was
604 identified by the strong asymmetry of the sample fabric: preferential growth on
605 the most highly illuminated side of the barrage was associated with the presence
606 of photoautotrophic microbes preserved as colonies of calcitic filament molds.
607 Though some calcite spar fans in this sample formed in association with microbial
608 filaments, the columnar spar that formed during a latter growth stage toward the

outside of specimen S3.2 does not include entombed microfossils. In contrast to speciment S3.2, the filaments found in the specimen Caerwys 1 were associated with the crystal structure of the deposit, which according to the criteria of Sugitani et al. (2007) and Wacey (2009), indicate that these structures are less plausible microfossil candidates than those found in S3.2.

Petrographic evidence indicates that columnar spar is a primary fabric, and not due to secondary crystal growth. This spar lacks obvious microfossils and formed within the calcite-precipitating stream, but in poorly illuminated locations behind the barrage front. Lamination is related to episodes of growth interrupted by intervals of non-deposition and erosion. We interpret the petrographic evidence as indicative of lamination formation controlled by physico-chemical parameters. Interestingly, we found that lamination in the samples studied was not an indicator of stromatolite biogenicity.

Acknowledgements

Natural Resources Wales and Steven Griffiths are thanked for access to Caerwys quarry and permission to work on the site. Sebastiaan Edelman and Thomas Logeman assisted with fieldwork and provided some of the field photographs.

628 Bouke Lacet (Sedimentology laboratory, VU University Amsterdam) prepared the
629 thin-sections. Three anonymous reviewers helped to sharpen the manuscript, and
630 Sherry Cady provided valuable editorial advice and assistance. ATB was inspired
631 by Martin Brasier. He dedicates this manuscript to his father's memory.

632

633 **Author Disclosure Statement**

634 No competing interests exist.

635

636 **References**

637 Andrews, J.E., Brasier, A.T., 2005. Seasonal records of climatic change in
638 annually laminated tufas: short review and future prospects. *Journal of*
639 *Quaternary Science* 20: 411-421.

640 Arp, G., Wedemeyer, N., Reitner, J., 2001. Fluvival tufa formation in a hard-
641 water creek (Deinschwanger Bach, Franconian Alb, Germany). *Facies* 44: 1-22.

642 Brasier, A.T., 2011. Searching for travertines, calcretes and speleothems in deep
643 time: Processes, appearances, predictions and the impact of plants. *Earth-Science*
644 *Reviews* 104: 213-239.

645 Brasier, A.T., 2007. Palaeoenvironmental Reconstructions from Quaternary Tufas
646 and Calcretes, central Greece. Unpublished Ph. D. thesis, University of East
647 Anglia, Norwich, UK. 294p.

648 Brasier, A.T., Andrews, J.E., Marca-Bell, A.D., Dennis, P.F. 2010. Depositional
649 continuity of seasonally laminated tufas: Implications for $\delta^{18}O$ based
650 palaeotemperatures. *Global and Planetary Change* 71: 160-167.

651 Brasier, A.T., Andrews, J.E., Kendall, A.C., 2011. Diagenesis or dire genesis?
652 The origin of columnar spar in tufa stromatolites of central Greece and the role of
653 chironomid larvae. *Sedimentology* 58: 1283-1302.

654 Buick, R., Dunlop, J., Groves, D., 1981. Stromatolite recognition in ancient rocks:
655 an appraisal of irregularly laminated structures in an Early Archaean chert-barite
656 unit from North Pole, Western Australia. *Alcheringa* 5: 161-181.

657 Cacchio, P., Contento, R., Ercole, C., Cappuccio, G., Martinez, M.P., Lepidi, A.,
658 2004. Involvement of microorganisms in the formation of carbonate speleothems
659 in the Cervo Cave (L'Aquila-Italy). *Geomicrobiology Journal* 21: 497-509.

660 Fairchild, I. J., Smith, C. L., Baker, A., Fuller, L., Spötl, C., Mattey, D., &
661 McDermott, F. (2006). Modification and preservation of environmental signals in
662 speleothems. *Earth-Science Reviews* 75: 105-153.

663 Freytet, P., Verrecchia, E.P., 1998. Freshwater organisms that build stromatolites:
664 a synopsis of biocrystallization by prokaryotic and eukaryotic algae.
665 *Sedimentology* 45: 535-563.

666 Frisia, S., Borsato, A., 2010. Karst. In *Carbonates in Continental Settings: Facies,*
667 *Environments, and Processes* edited by Alonso-Zarza, A.M. and Tanner, L.H.,
668 *Developments in Sedimentology* 61. Elsevier, Amsterdam.

669 Garnett, E., Andrews, J., Preece, R., Dennis, P., 2006. Late-glacial and early
670 Holocene climate and environment from stable isotopes in Welsh tufa.
671 *Quaternaire* 17: 31 - 42.

672 Gerbersdorf, S.U., Wieprecht, S. 2014. Biostabilization of cohesive sediments:
673 revisiting the role of abiotic conditions, physiology and diversity of microbes,
674 polymeric secretion, and biofilm architecture. *Geobiology* 13: 68-97.

675 Glunk, C., Dupraz, C., Braissant, O., Gallagher, K.L., Verrecchia, E.P., Visscher,
676 P.T., 2011. Microbially mediated carbonate precipitation in a hypersaline lake,
677 Big Pond (Eleuthera, Bahamas). *Sedimentology* 58: 720-736.

678 Grotzinger, J.P., Sumner, D.Y., Kah, L.C., Stack, K., Gupta, S., Edgar, D. et al.,
679 2014. A habitable fluvio-lacustrine environment at Yellowknife Bay, Gale Crater,
680 Mars. *Science* 343 (6169. doi: 10.1126/science.1242777

681 Niles, P.B., Catling, D.C., Berger, G., Chassefiere, E., Ehlmann, B.L., Michalski,
682 J.R., Morris, R., Ruff, S.W., Sutter, B. 2013. Geochemistry of carbonates on
683 Mars: Implications for climate history and nature of aqueous environments. *Space*
684 *Science Reviews* 174: 301-328.

685 Hammer, Ø., Dysthe, D.K., Jamtveit, B., 2010. Travertine terracing: patterns and
686 mechanisms. *Geological Society, London, Special Publication* 336: 345-355.

687 Hofmann, H., 2000. Archean stromatolites as microbial archives. In *Microbial*
688 *Sediments*.edited by Awramik, S.A., and Riding, R. Springer Berlin Heidelberg,
689 pp. 315-327.

690 Janssen, A., Swennen, R., Podoor, N., Keppens, E., 1999. Biological and
691 diagenetic influence in Recent and fossil tufa deposits from Belgium. *Sedimentary*
692 *Geology* 126: 75-95.

693 Jones, B., 2010. Microbes in caves: agents of calcite corrosion and precipitation.
694 *Geological Society, London, Special Publication* 336: 7-30.

695 Jones, B., Peng, X., 2012. Intrinsic versus extrinsic controls on the development
696 of calcite dendrite bushes, Shuzhishi Spring, Rehai geothermal area, Tengchong,
697 Yunnan Province, China. *Sedimentary Geology* 249: 45-62.

698 Kendall, A.C., Broughton, P.L., 1978. Origin of fabrics in speleothems composed
699 of columnar calcite crystals. *Journal of Sedimentary Petrology* 48: 519-538.

700 Knoll, A.H., Worndle, S, and Kah, L.C., 2013. Covariance of microfossil
701 assemblages and microbialite textures across an upper Mesoproterozoic carbonate
702 platform. *Palaios* 28: 453-470.

703 Love, K.M., Chafetz, H.S., 1988. Diagenesis of laminated travertine crusts,
704 Arbuckle Mountains, Oklahoma. *Journal of Sedimentary Research* 58: 441-445.

705 McLoughlin, N., Melezhik, V.A., Brasier, A.T., Medvedev, P.V. 2013.
706 Palaeoproterozoic stromatolites from the Lomagundi-Jatuli interval of the
707 Fennoscandian Shield. In: Melezhik, V.A. et al. (eds) Reading the Archive of
708 Earth's Oxygenation Volume 3: Global Events and the Fennoscandian Arctic
709 Russia – Drilling Early Earth Project. *Frontiers in Earth Sciences* 3:1298-1351.
710 Springer-Verlag, Berlin. doi: 10.1007/978-3-642-29670-3_8

711 Noffke, N., 2009. The criteria for the biogeneicity of microbially induced
712 sedimentary structures (MISS) in Archean and younger sandy deposits. *Earth-*
713 *Science Reviews* 96: 173-180.

714 Noffke, N., 2015. Ancient sedimentary structures in the <3.7 Ga Gillespie Lake
715 Member, Mars, that resemble macroscopic morphology, spatial associations, and
716 temporal succession in terrestrial microbialites. *Astrobiology* 15: 169-192.

717 Pedley, H., 1987. The Flandrian (Quaternary) Caerwys tufa, North Wales: an
718 ancient barrage tufa deposit. *Proceedings of the Yorkshire Geological Society* 46:
719 141-152.

720 Pedley, H.M., 1990. Classification and environmental models of cool freshwater
721 tufas. *Sedimentary Geology* 68: 143-154.

722 Pedley, M., 2014. The morphology and function of thrombolitic calcite
723 precipitating biofilms: A universal model derived from freshwater mesocosm
724 experiments. *Sedimentology* 61: 22-40.

725 Pedley, M., Rogerson, M., Middleton, R., 2009. Freshwater calcite precipitates
726 from *in vitro* mesocosm flume experiments: a case for biomediation of tufas.
727 *Sedimentology* 56: 511-527.

728 Preece, R.C., 1978. The biostratigraphy of Flandrian tufas in southern Britain.
729 Unpublished PhD thesis, University of London.

730 Preece, R.C., Turner, C., Green, H., 1982. Field excursion to the tufas of the
731 Wheeler Valley and to Pontnewydd and Cefn caves. Quaternary Research
732 Association Field Guide, London.

733 Preece, R., Turner, C., 1990. The tufas at Caerwys and Ddol. *North Wales Field*
734 *Guide* 162-166.

735 Rasmussen, B., Blake, T.S., Fletcher, I.R., Kilburn, M.R., 2009. Evidence for
736 microbial life in synsedimentary cavities from 2.75 Ga terrestrial environments.
737 *Geology* 37: 423-426.

738 Riding, R., 1991. Classification of microbial carbonates. In *Calcareous Algae and*
739 *Stromatolites*. Springer-Verlag, Berlin.

740 Rogerson, M., Pedley, H.M., Wadhawan, J.D., Middleton, R., 2008. New insights
741 into biological influence on the geochemistry of freshwater carbonate deposits.
742 *Geochimica et Cosmochimica Acta* 72: 4976-4987.

743 Rogerson, M., Pedley, H., Kelham, A., Wadhawan, J., 2014. Linking
744 mineralisation process and sedimentary product in terrestrial carbonates using a
745 solution thermodynamic approach. *Earth Surface Dynamics* 2: 197-216.

746 Sugitani, K., Grey, K., Allwood, A., Nagaoka, T., Mimura, K., Minami, M.,
747 Marshall, C.P., Van Kranendonk, M.J., and Walter, M.R., 2007. Diverse
748 microstructures from Archaean chert from the Mount Goldsworthy–Mount Grant
749 area, Pilbara Craton, Western Australia: microfossils, dubiofossils, or
750 pseudofossils? *Precambrian Research* 158: 228-262.

751 Wacey, D., 2009. Early Life on Earth: A Practical Guide. Springer.

752 Webster, C. R., Mahaffy, P.R. Atreya, S.K., Flesch, G.J., Mischna, M.A., et al.
753 Mars methane detection and variability at Gale crater. *Science* 347: 415-417.

754 Wright, V.P., Barnett, A.J., 2015. An abiotic model for the development of
755 textures in some South Atlantic early Cretaceous lacustrine carbonates. In
756 Bosence, D.W.J. et al. (eds) Microbial carbonates in space and time: Implications
757 for global exploration and production. Geological Society, London, Special
758 Publications 418, doi: 10.1144/SP418.3

759 Zhang, D.D., Zhang, Y., Zhu, A., Cheng, X., 2001. Physical Mechanisms of River
760 Waterfall Tufa (Travertine) Formation. *Journal of Sedimentary Research* 71: 205-
761 216.

762

763 **Figure captions**

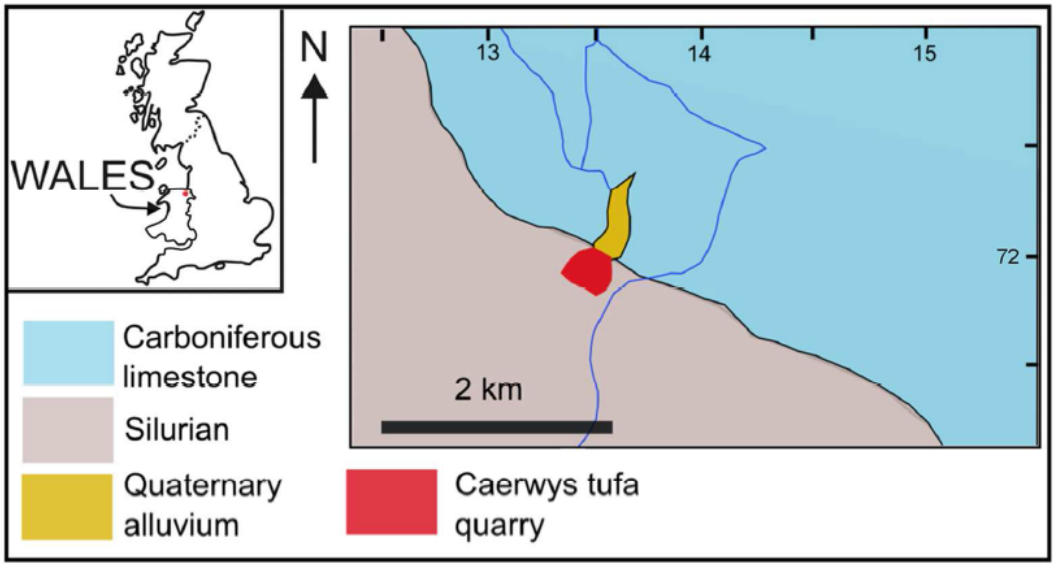

764
765 **FIG. 1:** Map showing the location of the Caerwys tufa in the UK. Inset map
766 shows the UK, with Wales labelled and Caerwys as a red dot. The larger map

767 shows the location of the Caerwys tufa quarry (red), and its relationship to
768 surrounding Quaternary alluvial sediments (orange) and underlying geology.
769 Carboniferous limestone (blue) supplies the calcium and bicarbonate ions to
770 groundwaters. These precipitate tufa calcite on emergence at springs associated
771 with the contact between the limestone and underlying Silurian siliciclastic rocks
772 (grey). Scale bar is 2km.

773

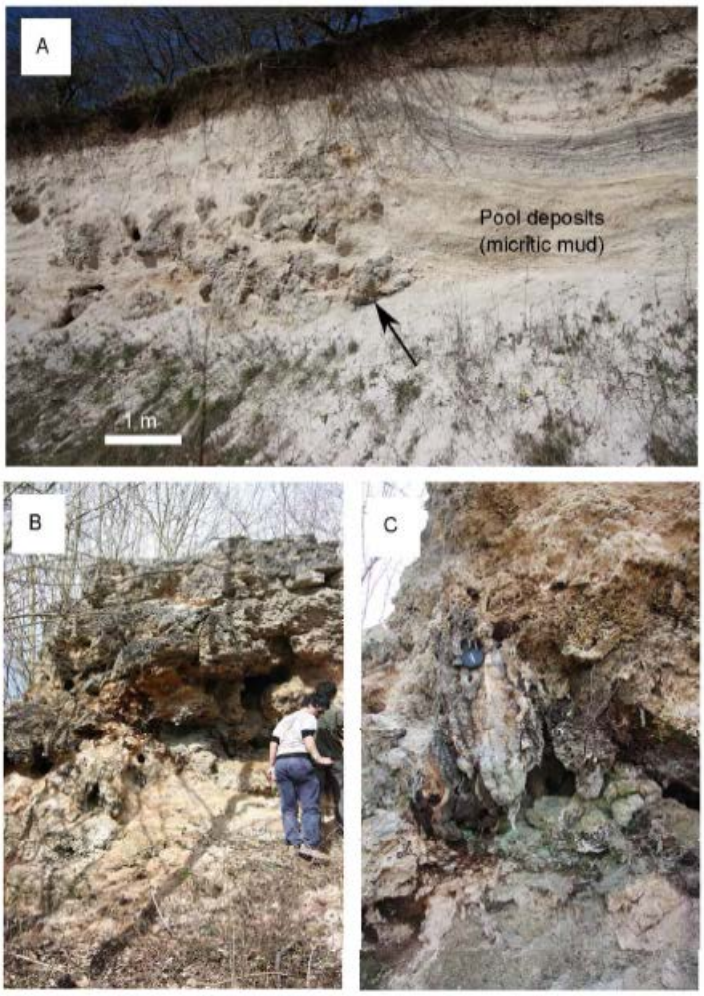

774

775 **FIG. 2:** Caerwys tufa quarry photographs **(a)** Unconsolidated micritic pool
776 deposits on the right side of the image, adjacent to consolidated barrage facies
777 (arrow points to the base of the barrage). The tufa barrage prograded downstream
778 (towards the left). Isolated thrombolitic heads are found in the pool facies. **(b)**
779 Block of the main tufa barrage preserved in the quarry center. People for scale are
780 c.1.75m tall. **(c)** Stalactitic carbonate rocks that grew in a cavity of the same

781 barrage block shown in (b). Specimen Caerwys 1 is from this location, and S3.2
782 was found as a float specimen nearby. Lens cap for scale is 5.5 cm diameter.

783

784

785 **FIG. 3:** Active tufa stream at Alport, Derbyshire, UK, as an analogue for the
786 Quaternary Caerwys tufa. **(a)** View showing pool environment behind a barrage
787 (to the right of this image), with a thrombolitic head (see arrow). The white water
788 upstream is flowing over a barrage. **(b)** Close-up of a barrage, showing microbial

biofilm plus some green algae and bryophytes living subaqueously on the barrage front, hanging down into the fast flowing stream. A cavity is developing behind this calcifying structure sometimes referred to as a curtain. In larger barrages, meter-scale caverns form behind the curtain (e.g., fig. 2c).

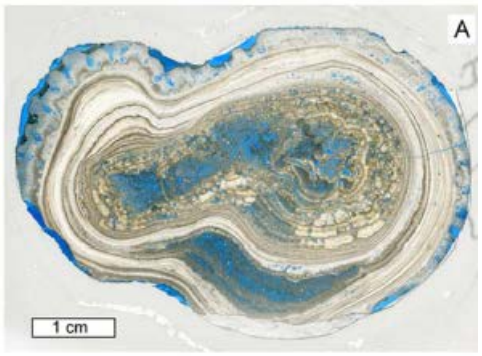

794 **FIG. 4:** Scans of thin-sections of specimen S3.2. **(a)** transverse cut, and **(b)**

795 longitudinal cut. Blue color is from resin injected to show porosity.

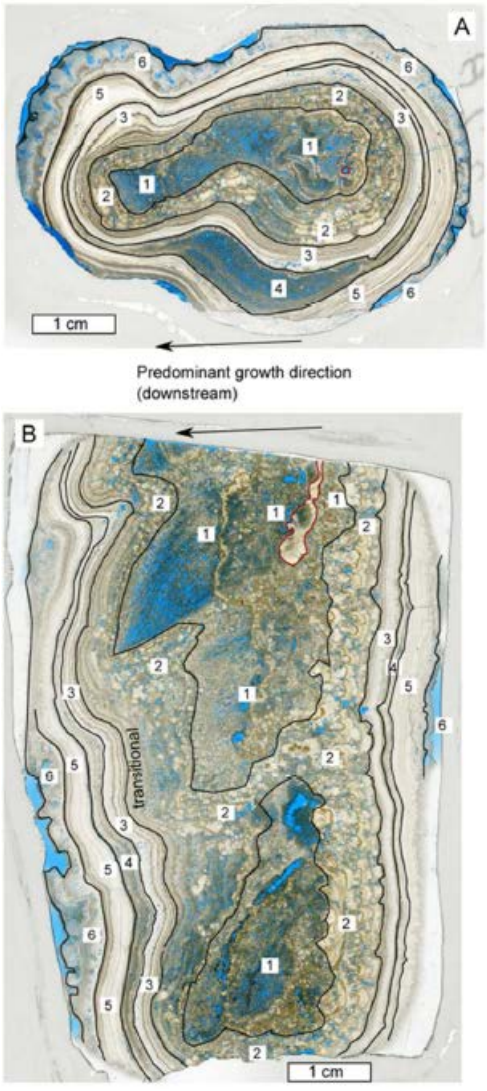

796

797 **FIG. 5:** Interpreted scans of thin-sections of specimen S3.2. **(a)** transverse cut and

798 **(b)** longitudinal cut. Interpreted boundaries between growth zones are shown as

799 black lines, and the position from which growth initiated is shown as a red line.

800 Zones 1-6 are described in the text. Unlike wholly abiotic stalactites, this
801 specimen is strongly asymmetrical, caused by calcifying cyanobacteria favoring
802 the illuminated side of the specimen. Images are shown at the same scale.

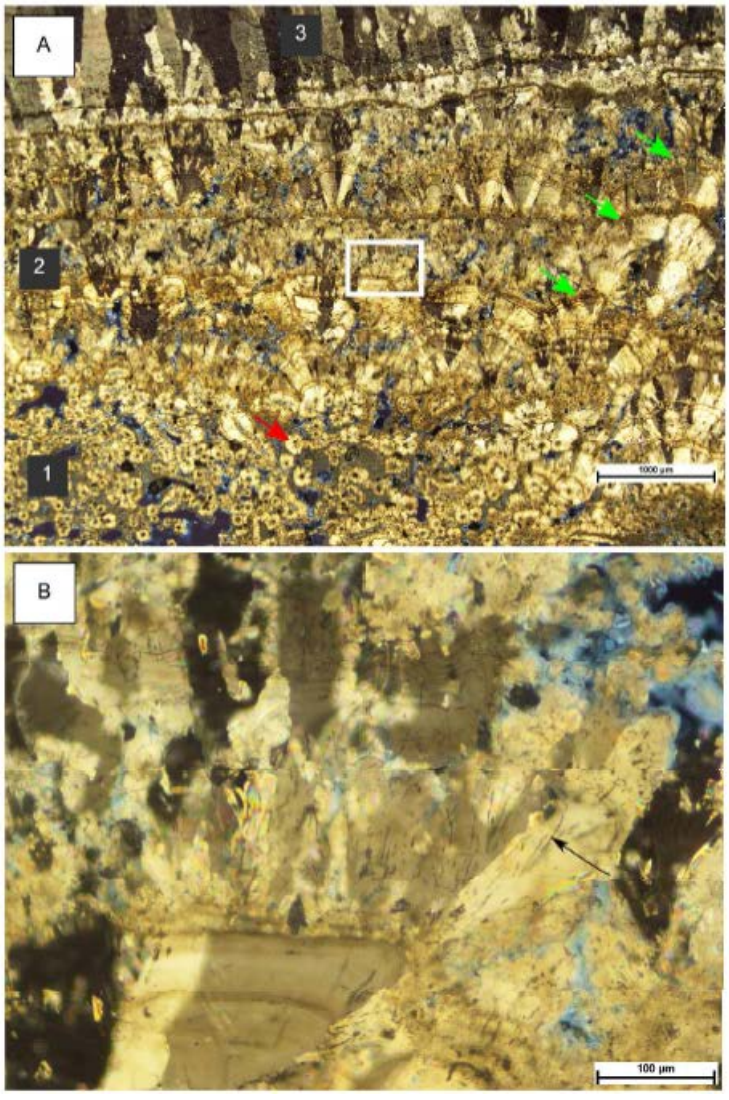

803

804 **FIG. 6:** Micrographs of Specimen S3.2 thin-section A (transverse cut). **(a)** shows
805 Zone 1 (base, hollow calcite tubes that formed around downward-hanging

cyanobacterial filaments; example arrowed), Zone 2 (center, sparry calcite fans interlayered with micritic bands) and Zone 3 (top, columnar calcite crystals). Numbered squares refer to these zones. Green arrows point to cessations in growth, marked by dark micritic layers, from which new fans nucleated. White box in Zone 2 shows location of **(b)**, which is a sparry calcite fan that contains entombed cyanobacterial filaments (arrowed).

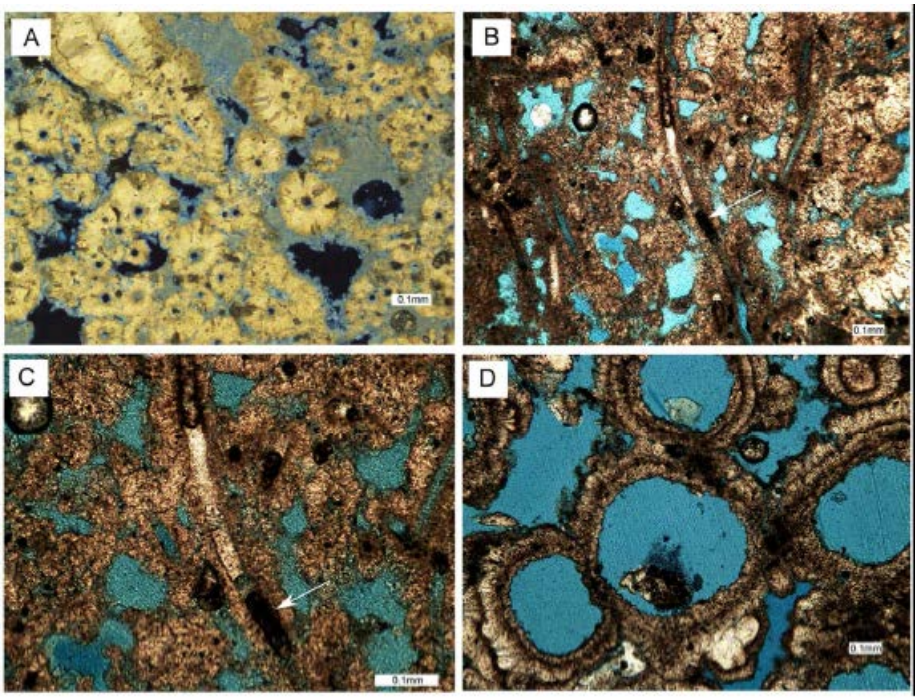

FIG. 7: Micrographs of Specimen S3.2 showing biological fabrics. **(a)** Cross-polarized light image of Zone 1 calcite tubes formed around downward-hanging cyanobacterial filaments (transverse cut). Blue is resin, and black is holes in the

thin-section. **(b)** Plane polarized light image of calcite tubes containing microfossils of filamentous cyanobacteria (longitudinal cut). Trichome in a sheath is arrowed. **(c)** Higher magnification plane polarized light image of the trichome and sheath shown in (b). **(d)** Plane polarized light image of a network of larger diameter calcite-cemented holes best interpreted as insect (interpreted as chironomid?) larval tubes.

FIG. 8: A sparry calcite fan containing entombed cyanobacterial filaments of specimen S3.2 Zone 2. Note the filaments are dominantly oriented parallel to the direction of crystal growth. However they also curve and cross each other, and are not artifacts related to the crystal structure. Filaments also cross dark colored

growth banding (likely formed on ~diurnal timescales) in the crystal. Scale bar is 0.1 mm across.

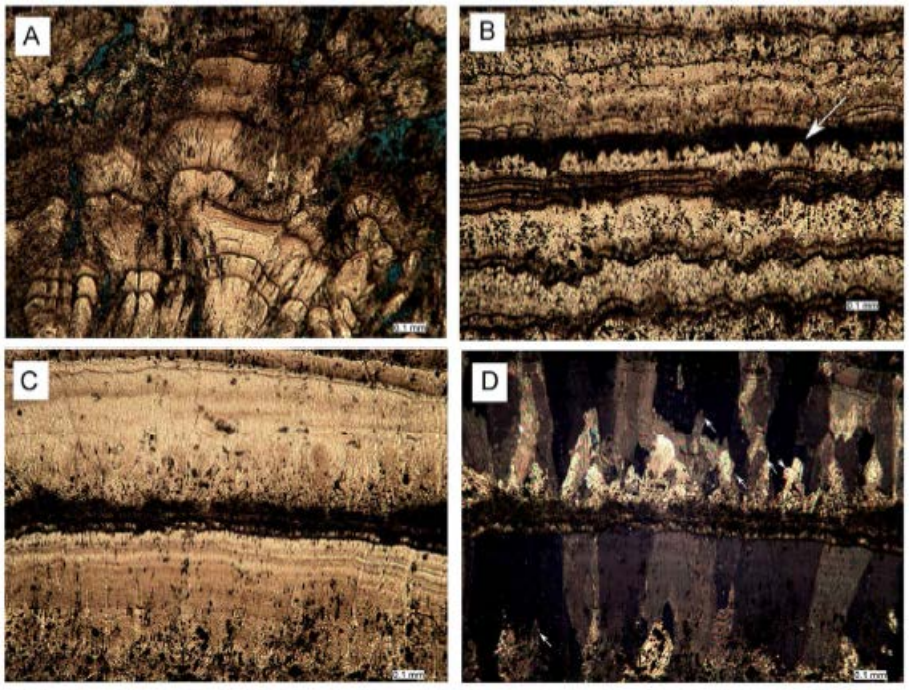

FIG. 9: Sparry calcite of Specimen 3.2 Zone 3. **(a)** shows the top of Zone 2, transitioning into Zone 3. Note the shrub-like calcite crystal fans with entombed cyanobacterial filaments of Zone 2. **(b)** shows alternating laminae of calcite spar and micrite of Zone 3. The arrow points to a partially broken pointed termination of a spar crystal draped in dark micrite. **(c)** shows (apparently abiotic) sparry calcite laminae found further from the specimen center than (b), with dusty lamination caused by inclusions. **(d)** is the same area as (c), with polars crossed. Note competitive growth has favored some crystals over others, resulting in a

columnar fabric. Examples of crystals that were out-competed are arrowed. Note also that new crystals nucleated on the micrite layers (presumed hiatuses in growth), consistent with this columnar spar being a primary fabric.

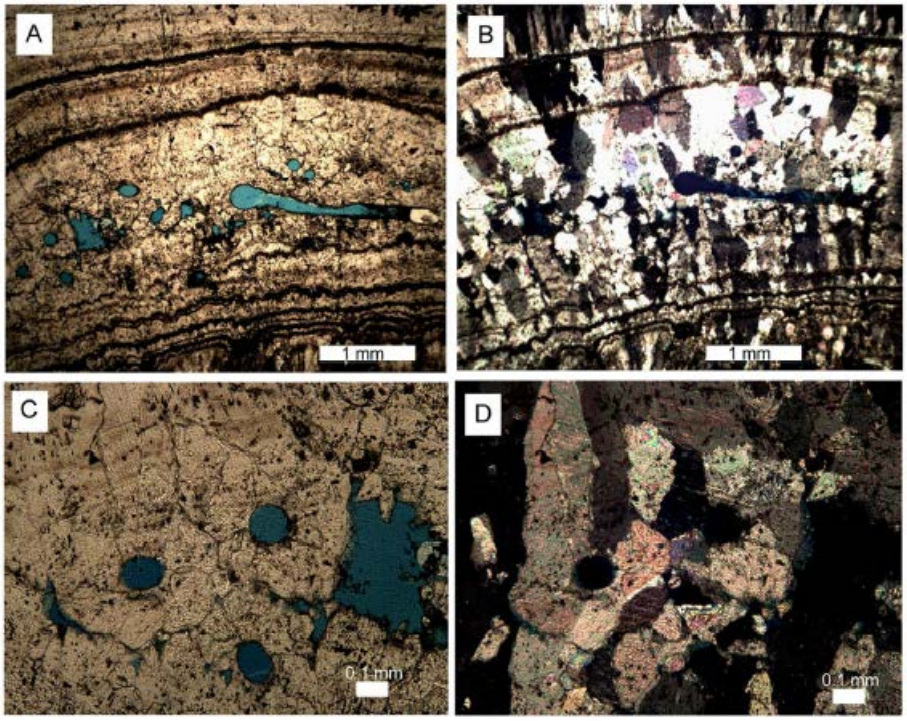

FIG. 10: Insect (likely chironomid) larval tubes in Specimen S3.2 Zone 3 spar. These are seen as evidence that the spar is primary and not recrystallized from micrite. **(a)** plane polarized light image, showing hollow tube (filled with blue resin) within the spar of Zone 3. **(b)** Same area as (a), with polars crossed. Note the influence of the insect larvae on crystal orientations. **(c)** Close up of some of the tubes in plane polarized light. **(d)** Same area as (c), with polars crossed. Some crystal orientations seem consistent with the broader columnar fabric of Zone 3.

850 Crystals with different orientations might have been detrital grains assimilated by
851 the larvae for tube construction.

852

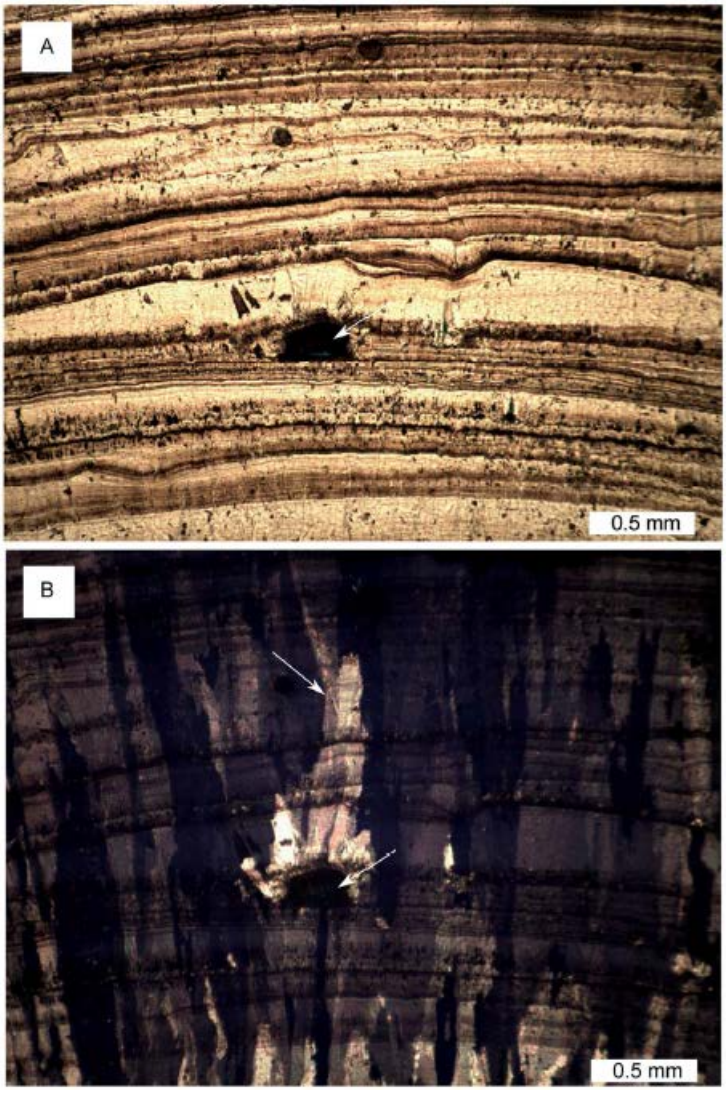

853

FIG. 11: Caerwys specimen 3.2 Zone 5 in thin-section. **(a)** Plane polarized light image, showing sparry crystals (light) with dark micritic growth laminae. Arrow points to a micritic grain that stuck to the specimen surface during growth, and became enveloped in (primary) columnar spar. **(b)** Same area as (a) with polars crossed. Note the influence of the detrital micrite clast (lower arrow) on columnar spar growth. Crystals nucleated on the micrite were out-competed by the larger columnar crystals (top arrow). This suggests the columnar spar was primary, despite the fact that these large crystals cut through the dusty growth lamination.

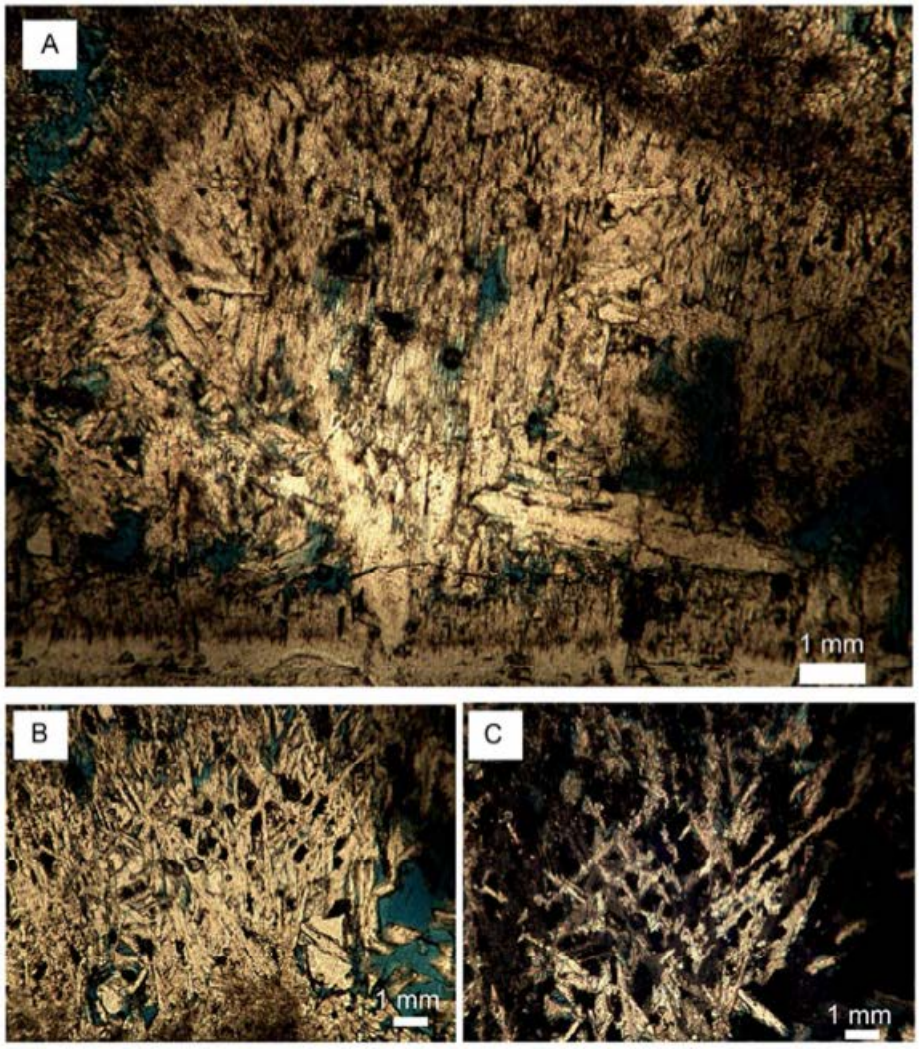

FIG. 12: Caerwys specimen 3.2 Zone 6 in thin-section. **(a)** Plane polarized light image showing a mound of crystal laths nucleated on a flat surface (the top of a Zone 5 columnar calcite crystal, at the base of the image). **(b)** Close up of network of lath-shaped crystallites in plane polarized light. **(c)** Image with polars crossed, showing the network of lath-shaped crystallites forms composite crystals of Zone 6. All scale bars are 1 mm.

870

871

872 **FIG. 13:** Stalactitic specimen Caerwys 1 (longitudinally cut hand-specimen). The
873 central cavity formed around a downward-hanging twig. Alternating micritic
874 laminae (white) and sparry calcite fans (darker and thicker) grew on the outside.

875 Ruler for scale (larger divisions are centimeters, smaller divisions are

876 millimeters).

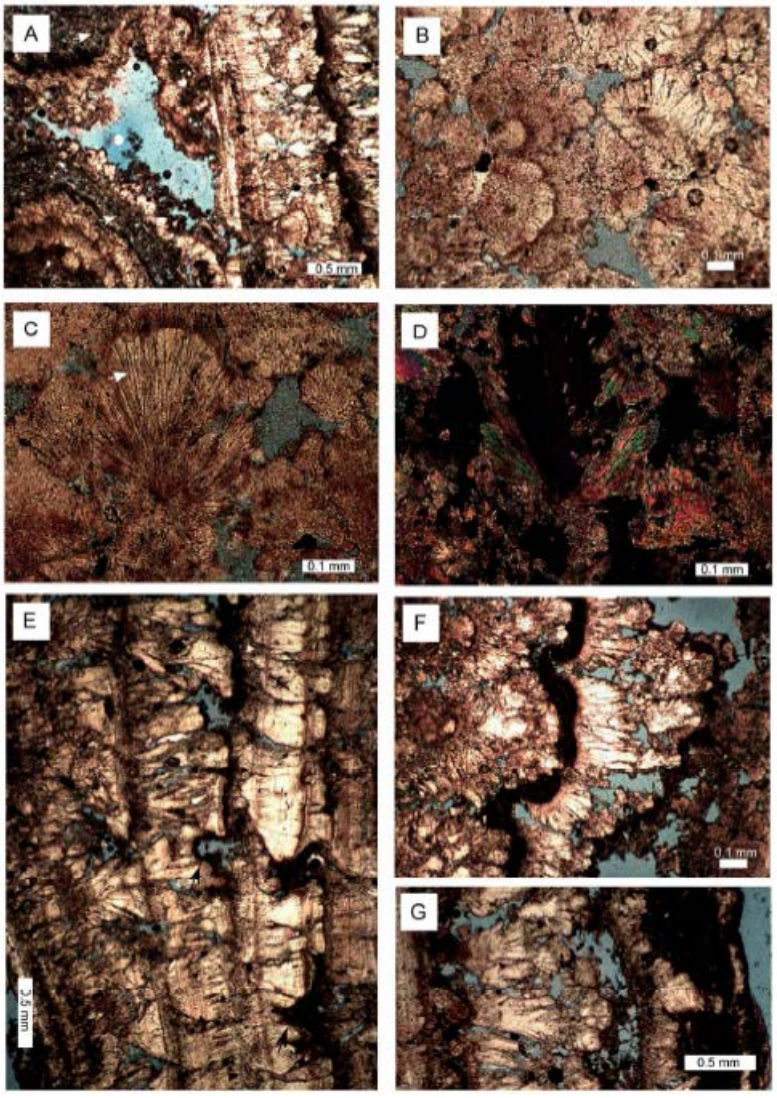

877

878

FIG. 14: Photomicrographs of Caerwys 1 thin-section. **(a)** The central cavity region is highly porous, with several hollow, empty pockets (blue resin). The empty pocket in (a) is lined with 20µm diameter microspar crystals. These grew on peloidal micrite (arrowed). **(b)** A second empty pocket in the central zone, 3 mm across, that has been progressively filled by 300 µm diameter sparry calcite fans. **(c)** Inclusions within these fans (arrowed), oriented along crystallite boundaries. Their alignment and form suggest they are not cyanobacterial and possibly not even microbial filaments. **(d)** Same crystal fan as shown in (c), with polars crossed. **(e)** Layers of columnar sparry calcite growing dominantly outward as fans that form the bulk of the specimen. There is evidence that columnar sparry calcite fans were partially dissolved prior to or during deposition of the micrite layers. **(f)** Close-up of one of the micritic laminae (dark band) between sparry calcite fans. **(g)** Sparry calcite fans on the left, capped by a thick micrite layer (dark band on the right) close to the outside of the specimen. All images taken in plane polarized light except (d). Scale bars in (a), (e), and (g) are 0.5mm; scale bars in other images are 0.1 mm.